





Article

Glycerolized Li⁺ Ion Conducting Chitosan-Based Polymer Electrolyte for Energy Storage EDLC Device Applications with Relatively High Energy Density

Ahmed S. F. M. Asnawi ¹, Shujahadeen B. Aziz ^{2,3,*} , Muaffaq M. Nofal ⁴ ,
Muhamad H. Hamsan ⁵, Mohamad A. Brza ^{2,6}, Yuhanees M. Yusof ⁷, Rebar T. Abdilwahid ² ,
Saifful K. Muzakir ⁸  and Mohd F. Z. Kadir ⁹

- ¹ Chemical Engineering Section, Malaysian Institute of Chemical & Bioengineering Technology (UniKL MICET), Universiti Kuala Lumpur, Alor Gajah 78000, Malacca, Malaysia; asyafiq.asnawi@s.unikl.edu.my
 - ² Hameed Majid Advanced Polymeric Materials Research Laboratory, Department of Physics, College of Science, University of Sulaimani, Qlyasan Street, Kurdistan Regional Government, Sulaimani 46001, Iraq; mohamad.brza@gmail.com (M.A.B.); rebar.abdulwahid@univsul.edu.iq (R.T.A.)
 - ³ Department of Civil Engineering, College of Engineering, Komar University of Science and Technology, Kurdistan Regional Government, Sulaimani 46001, Iraq
 - ⁴ Department of Mathematics and General Sciences, Prince Sultan University, P.O. Box 66833, Riyadh 11586, Saudi Arabia; muaffaqnofal@gmail.com
 - ⁵ Institute for Advanced Studies, University of Malaya, Kuala Lumpur 50603, Malaysia; hafizhamsan93@gmail.com
 - ⁶ Department of Manufacturing and Materials Engineering, Faculty of Engineering, International Islamic University of Malaysia, Kuala Lumpur, Gombak 53100, Malaysia
 - ⁷ Malaysian Institute of Chemical and Bio-Engineering Technology, Universiti Kuala Lumpur (UniKL MICET), Alor Gajah 78000, Malacca, Malaysia; yuhanees@unikl.edu.my
 - ⁸ Material Technology Program, Faculty of Industrial Sciences & Technology, Universiti Malaysia Pahang, Lebuhraya Tun Razak, Gambang, Kuantan 26300, Pahang, Malaysia; saifful@ump.edu.my
 - ⁹ Centre for Foundation Studies in Science, University of Malaya, Kuala Lumpur 50603, Malaysia; mfzkadir@um.edu.my
- * Correspondence: shujahadeenaziz@gmail.com or shujaadeen78@yahoo.com

Received: 31 May 2020; Accepted: 23 June 2020; Published: 26 June 2020



Abstract: In this study, the solution casting method was employed to prepare plasticized polymer electrolytes of chitosan (CS):LiCO₂CH₃:Glycerol with electrochemical stability (1.8 V). The electrolyte studied in this current work could be established as new materials in the fabrication of EDLC with high specific capacitance and energy density. The system with high dielectric constant was also associated with high DC conductivity (5.19×10^{-4} S/cm). The increase of the amorphous phase upon the addition of glycerol was observed from XRD results. The main charge carrier in the polymer electrolyte was ion as t_{el} (0.044) < t_{ion} (0.956). Cyclic voltammetry presented an almost rectangular plot with the absence of a Faradaic peak. Specific capacitance was found to be dependent on the scan rate used. The efficiency of the EDLC was observed to remain constant at 98.8% to 99.5% up to 700 cycles, portraying an excellent cyclability. High values of specific capacitance, energy density, and power density were achieved, such as 132.8 F/g, 18.4 Wh/kg, and 2591 W/kg, respectively. The low equivalent series resistance (ESR) indicated that the EDLC possessed good electrolyte/electrode contact. It was discovered that the power density of the EDLC was affected by ESR.

Keywords: chitosan; glycerol plasticizer; electrical properties; impedance study; EDLC fabrication

1. Introduction

Renewable energy and high-performance energy devices are required for the human lifestyle because of the increasing demand for a clean environment [1]. Recently, an electrochemical double-layer capacitor (EDLC) emerges as a potential alternative for conventional batteries and even fuel cells. The principle of energy storage mechanism in this device is based on the non-Faradaic process, where the ions accumulate at the interfacial region in the form of a double-layer [2]. This means only charge accumulation occurs between the electrode surfaces and the bulk electrolyte, and there is no electron transfer (i.e., Faradaic process). Based on the relatively high power density, durability, and thermal stability, EDLC is superior over supercapacitors. It is also taken into consideration that the cost-effectiveness and straightforwardness of the fabrication of EDLC are of significant importance in terms of technological aspects [2–4]. For EDLC fabrication, the electrodes have been made from several materials, such as graphite [5], carbon aerogel [6], carbon nanotubes [7], and activated carbon [8]. The activated carbon is intensively and extensively utilized as characterized by a large surface area, satisfactory chemical stability, and high electronic conductivity [9]. Another component in EDLC design is the electrolyte between the electrodes where solid polymer electrolytes (SPEs) with conductivity between $\sim 10^{-4}$ and 10^{-3} Scm^{-1} have been used. A few attempts have been introduced to improve the conductivity of such electrolytes, for instance, salt impregnation and plasticization [10,11]. Gupta et al. [12] studied the conductivity of hydroxyl ethyl cellulose film, which was increased up to $3.8 \times 10^{-5} \text{ Scm}^{-1}$ and $4.4 \times 10^{-3} \text{ Scm}^{-1}$ with the addition of 0.5 wt.% lithium tetraborate ($\text{Li}_2\text{B}_4\text{O}_7$) salt and 20 wt.% glycerol, respectively. In another study, there has been an increase in conductivity of dextran-ammonium nitrate (NH_4NO_3) system from $3.00 \pm 1.60 \times 10^{-5} \text{ Scm}^{-1}$ to $1.15 \pm 0.08 \times 10^{-3} \text{ Scm}^{-1}$ with 20 wt.% of glycerol addition [13]. The critical step in increasing conductivity depends upon the plasticization process, which facilitates the degree of dissociation of salts [14]. The liquid electrolytes are widely used because of their high performance in various energy devices despite the ease of evaporation and leakage, which causes corrosion [15,16]. However, the SPEs have several advantages compared to liquid electrolyte counterparts, such as safety and ease of fabrication, as well as long shelf life [17]. There are two categories of polymer hosts—natural and synthetic polymers. These are commonly documented in the synthesis of SPEs that are used in electrochemical energy devices [18]. The synthetic polymers are non-biodegradable that impact petroleum resources; hence, it is detrimental to the environment [19]. In terms of biodegradability, the synthetic polymers as a polymer host in the study of energy storage devices have been utilized over the last decades. Thereby, less plastic waste pollutants will release into the environment. The natural polymers and biopolymers are used interchangeably, are typically characterized by cost-effectiveness, high compatibility with solvents, high capability in film-forming, and natural abundance [20,21]. For example, starch, cellulose, and carrageenan are most commonly used as polymer hosts [22–24]. Another common biopolymer that is extensively under intensive investigation in energy storage devices is chitosan [25]. This biopolymer enriches in various oxygen-containing functional groups (i.e., availability of non-bonding electron pair) based on chemical structure. The problem of low conductivity in chitosan is solved by salt incorporation, where the mechanism of conduction is significantly affected. The ions from the incorporated salts are in sufficient contact with functional groups within the polymer body that provide dative bond [26]. Recently, it has been shown that the addition of glycerol accompanying specific lithium salt into chitosan-based polymer electrolyte improves conductivity. Such a conducting electrolyte system has been employed in EDLC fabrication.

2. Materials and Methods

2.1. Materials

In the present work, chitosan with a relatively high molecular mass of around 310,000 to 375,000 g/mol along with glycerol in the fabrication of plasticized systems was used as received. Both chemicals were purchased from Sigma-Aldrich (Missouri, MO, USA).

2.2. Polymer Electrolyte Preparation

The procedure involved the addition of 1 g of Chitosan (CS) into 50 mL of acetic acid (1%) solution. Afterward, a constant weight ratio (40 wt.%) of lithium acetate (LiCO_2CH_3) salt was added to the previous solution. The solution was stirred continuously with the magnetic stirrer at room temperature until a homogenous solution was obtained. Then, a various weight percentage ratio of glycerol was added to the polymer-salt mixture, with stirring continuously until a clear solution was gained. The percentage of glycerol content in the prepared samples varied from 14 to 42 wt.%. The samples were then coded as CSGL1, CSGL2, and CSGL3 for CS: LiCO_2CH_3 electrolyte incorporated with 14 wt.%, 28 wt.%, and 42 wt.% of glycerol, respectively. Finally, the solutions were then spilled into different clean and dry glass Petri dishes, covered with filter paper to prevent any contamination. The Petri dishes were left to evaporate solvent slowly at room temperature, to obtain dry and a free-standing plasticized CS polymer electrolyte films.

2.3. Impedance and X-Ray Diffraction (XRD) Studies

To investigate the electrical properties of the films, the electrochemical impedance spectroscopy (EIS) [HIOKI, 3532–50 LCR HiTESTER, Hioki, Nagano, Japan] from 50 Hz to 5 MHz was employed for receiving the impedance spectra of the samples. D5000 X-ray diffractometer (1.5406 \AA) [Bruker AXS GmbH, Berlin, Germany] was used for the structural study of the polymer films. The scanning angle of the films was set in the range of 10° to 80° (resolution = 0.1°).

2.4. Transference Number (TNM) and Linear Sweep Voltammetry (LSV) Measurements

The digital DC power supply, V&A Instrument (Neware, Shanghai, China) DP3003, was employed to perform the transference number (TNM) analysis from the DC polarization technique. Before starting measurements, the relatively high conducting electrolyte was sandwiched between blocking stainless steel electrodes in a Teflon holder. The electrode polarization was carried out by holding potential at 0.8 V, and the DC current was recorded as a function of time at room temperature. The potential window of the conducting electrolyte was also determined using linear sweep voltammetry (LSV) analysis (DY2300 potentiostat, Neware, Shenzhen, China) at a scan rate of 10 mV/s. The image of the fabricated SPE is indicated in Figure 1a, and the circle image of the SPE after LSV examination is shown in Figure 1b. It is seen in Figure 1b that the SPE film was oxidized beyond the decomposition voltage.

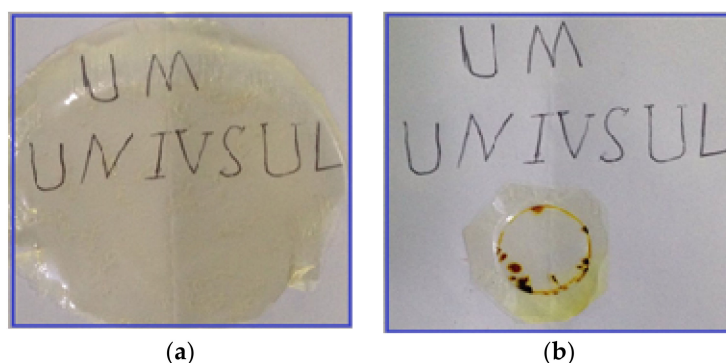


Figure 1. (a) Image of the fabricated solid polymer electrolyte (SPE). (b) Circle image of the fabricated SPE after linear sweep voltammetry (LSV) examination.

2.5. EDLC Preparation

The electrode made of polyvinylidene fluoride (PVdF), activated carbon, and carbon black materials was used in the EDLC study. The detail of the electrode preparation can be seen in our

previous work [2]. The thickness of the electrodes varied to obtain an optimum of 25 μm . The specific capacitance (C_s) was calculated from the CV response using the following relation [27]:

$$C_{spe} = \int_{V_i}^{V_f} \frac{I(V)dV}{2mv(V_2 - V_1)} \quad (1)$$

where $\int I(V)dV$ is the area of the CV curve, which was determined using Origin 9.0 software; m and v are the mass of active material and scan rate, respectively. The potential range of 0.9 V to 0 V from starting (V_2) to the ending (V_1), respectively, was applied. The charge-discharge profiles of the system were tested using a Neware battery cycler with a current density of 0.5 mA/cm². The specific capacitance (C_s) from charge-discharge profiles and equivalent series resistance (ESR) were calculated using the Equations shown below [28,29]:

$$C_s = \frac{i}{sm} \quad (2)$$

$$ESR = \frac{V_d}{i} \quad (3)$$

where i is the applied current, s is the slope of discharge part, and V_d is the voltage drop.

3. Results and Discussion

3.1. Dielectric Properties

To deal with ionic transport phenomenon in the SPEs, it is of the best choice to analyze the dielectric relaxation. From this analysis, one can examine the nature and ionic movement of polymer-plasticizer interactions [30,31]. To tackle dielectric properties, there are several parameters, such as relative permittivity, loss tangent, dielectric constant, microwave reflection coefficient, split post dielectric resonance technique, and terahertz material [31]. The dielectric constant or complex permittivity is defined by the following mathematical relation [32]:

$$(\epsilon^*) = \epsilon' - j\epsilon'' \quad (4)$$

where ϵ' is the real dielectric constant, and ϵ'' is the imaginary dielectric loss, which essentially specifies the energy loss and storage in every cycle of the applied power supply [30]. Both the real and imaginary parts of complex permittivity (ϵ^*) are calculated from the impedance data (i.e., Z' and Z'') using the Equations presented below [33,34],

$$\epsilon' = \left[\frac{Z''}{\omega C_0(Z'^2 + Z''^2)} \right] \quad (5)$$

$$\epsilon'' = \left[\frac{Z'}{\omega C_0(Z'^2 + Z''^2)} \right] \quad (6)$$

where ω is the angular frequency of the applied field ($\omega = 2\pi f$), and ϵ' and ϵ'' are the dielectric constant and dielectric loss, respectively. The C_0 is the vacuum capacitance given by $\epsilon_0 A/t$, ϵ_0 is the permittivity of free space, A is the electrode cross-sectional area, and t is the film thickness. Figures 2 and 3 show the real and imaginary part of dielectric constant (ϵ' , ϵ'') as a function of frequency at room temperature. It is observable that the value of ϵ' rises very sharply for the high amount of glycerol plasticizer at the low-frequency region as a result of the influence of space charge and electrode polarization (EP) [35]. At the electrode/electrolyte interfacial region, a high concentration of charge carriers accumulated because of the increase in the polarization in the low frequency [36]. At the higher frequency regions, it is clearly seen that there is no possibility of excess ion dispersion to align with the direction of the field as the consequence of the periodic reversal of the electric field takes place rapidly. Regarding both dielectric constant and dielectric loss, there is a decrease in the values due to the polarity declination [37].

It is known that the carrier density is in strong association with the dissociation energy (U) as well as dielectric constant (ϵ'), which can be formulated in this relationship ($n = n_o \exp(-U/\epsilon'KT)$).

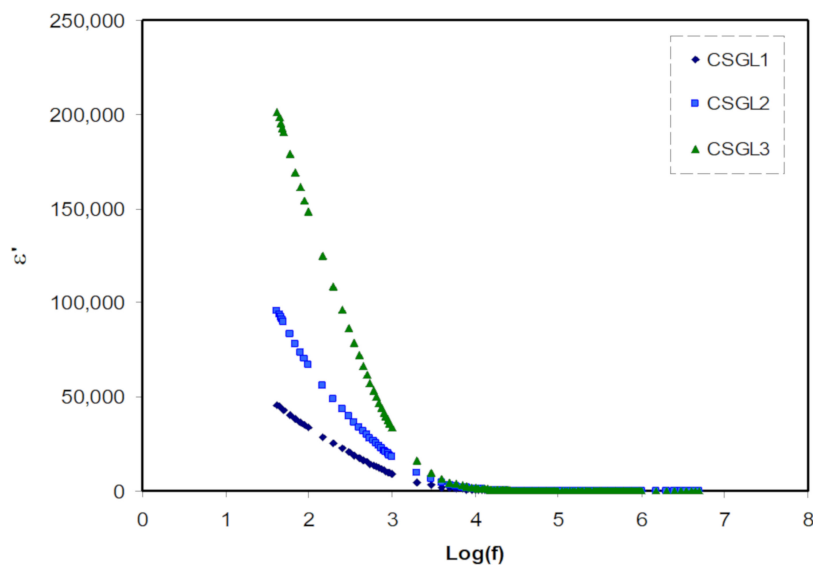


Figure 2. Dielectric constant versus log (f) for all polymer blend electrolytes.

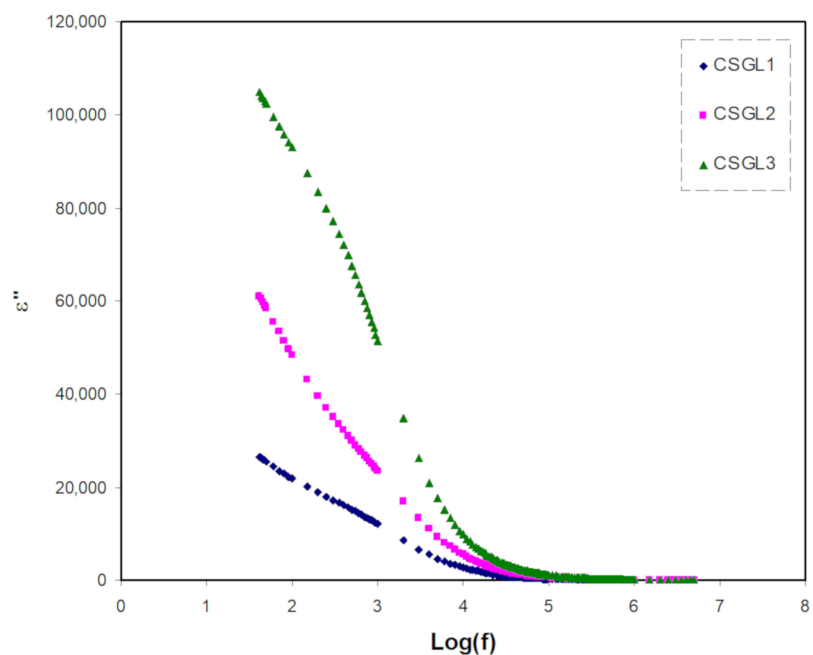


Figure 3. Dielectric loss versus log (f) for all polymer blend electrolytes.

The value of dielectric constant increases with the increasing salt concentration and there is a substantial increase in the number of charge carriers and thus a rise in DC conductivity [38–41]. To investigate and comprehend the SPEs’ conductivity behavior, it is best to measure DC conductivity and dielectric constant, as well as a function of the concentration of the salt at room temperature.

3.2. Impedance Study

Impedance spectroscopy is a powerful technique to be used in examining the ionic conductivity of polymeric materials [42–44]. Electrochemical impedance spectroscopy (EIS) is also used as an impressive technique to analyze electrical properties of the new materials that are utilized in electrochemical energy devices, for example, double-layer capacitance, diffusion layer, and charge transfer resistance [39].

Over the previous decade, the ion-conducting membrane is a class of materials, which have attracted attention owing to the wide applications in solid electrochemical devices [42]. The EIS responses of polymer electrolytes commonly consist of a semicircle and a spike at high and low-frequency regions, respectively [43]. The semicircle results from charge transfer at the interface. On the contrary, similar behavior is not obtained in the measurement of the EIS, as presented in Figure 4a–c. At the low-frequency region, the spike region arises owing to EP (that is, the effect of blocking electrodes). The EP phenomenon occurs as a result of the growth of electric double-layer, as a consequence of free charge accumulation at the solid electrolyte and electrode interface [45,46]. Accordingly, at the low frequency, it is supposedly for the complex impedance to show a straight line parallel to the imaginary axis. In other words, the straight line’s inclination ought to be 90°, and the blocking double-layer capacitance (EP phenomena) at the blocking electrodes is responsible for the inclination [47,48]. The ionic conductivity of the CS:LiCO₂CH₃:Gly systems can be calculated using the following Equation [49]:

$$\sigma_{dc} = \left(\frac{1}{R_b}\right) \times \left(\frac{t}{A}\right) \tag{7}$$

where t is the thickness of the sample, R_b is the bulk resistance of the material, and A is the area of the electrode [50,51]. It is of vital importance to determine the DC conductivity of the samples from the R_b value using the above Equation.

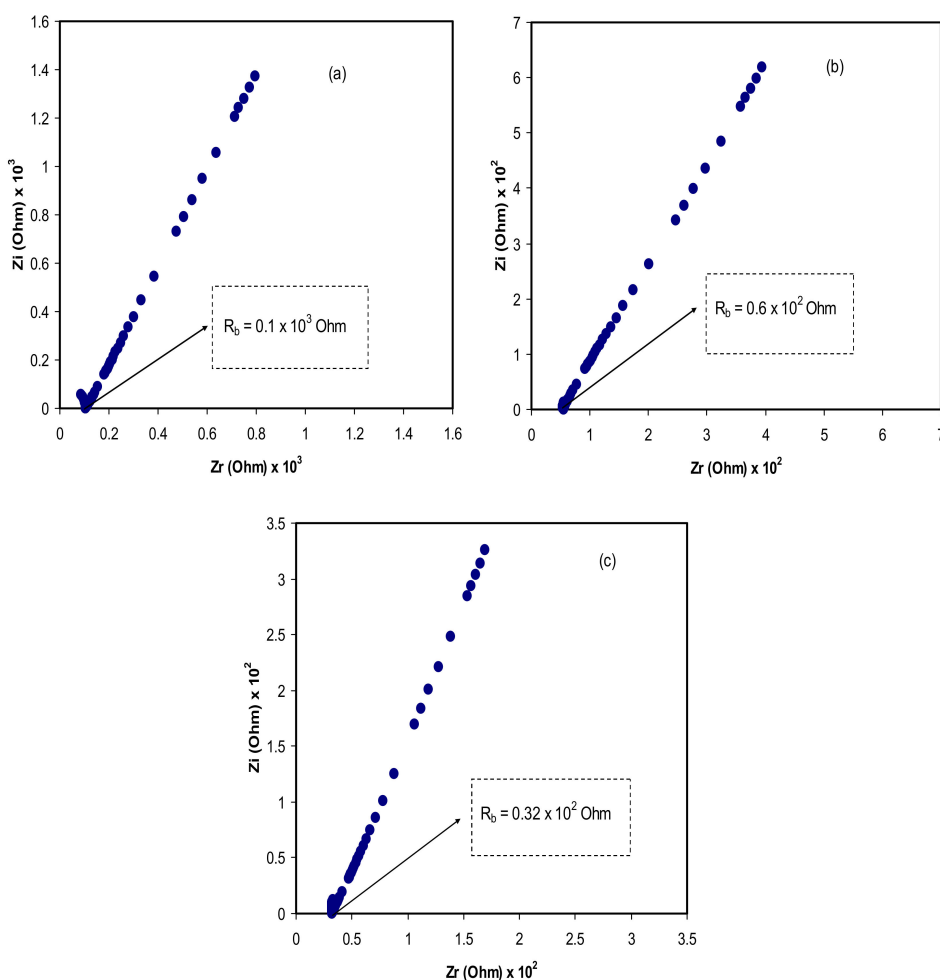


Figure 4. Complex impedance plots for (a) CSGL 1, (b) CSGL 2, and (c) CSGL 3.

The DC conductivities are calculated and tabulated, as shown in Table 1. It is seen that the highest ionic conductivity is recorded for lower bulk resistance R_b material, with $5.19 \times 10^{-4} \text{ Scm}^{-1}$. Therefore,

one reason behind employing polymer blend electrolytes in practical usage in electrical double-layer capacitors (EDLCs) is a relatively high DC conductivity. The dependency of conductivity of electrolytes on the number density and the mobility of the ions is well-known and has been mathematically shown [40,50]:

$$\sigma = \sum \eta q \mu \quad (8)$$

where η denotes the carrier density, q denotes simple charge, and μ represents mobility. An earlier study has suggested that the charge species of Li^+ ion is released by lithium salt within the polymer-lithium salt system [51]. Table 1 shows the DC conductivity values of electrolyte samples at ambient temperature. From Figure 4, it is seen that there is a decrease in the bulk resistance with increasing plasticizer concentration from 14 to 42 wt.%. It has also been confirmed that it is essential for polymer electrolytes to be used in electrochemical device applications, such as batteries and EDLCs, if the DC conductivity lies between 10^{-5} and $10^{-3} \text{ S cm}^{-1}$ [52,53]. It is worth-mentioning that glycerol is helpful in improving DC conductivity in polymer electrolytes when plasticized. The more insight into the influence of glycerol as a plasticizer in polymer electrolytes has been discussed in the next section.

Table 1. Calculated DC conductivity for CS: LiCO_2CH_3 :Gly electrolyte films at room temperature.

Sample Designation	DC Conductivity (S/cm)
CSGL1	1.66×10^{-4}
CSGL2	2.77×10^{-4}
CSGL3	5.19×10^{-4}

3.3. XRD Analysis

It is known that in the preparation of a polymer electrolyte, pure polymer materials consist of a mixture of amorphous and crystalline phases [41,51]. It is of great importance to determine the degree of crystallinity in a polymer structure using an accurate method. Therefore, the determination of crystallinity is not only useful in determining the molecular structure of a crystalline polymer but also in comprehensive understanding and rationalizing the intrinsic properties of polymeric materials [31]. In the previous work, it has been emphasized that chitosan (CS) possesses a range of crystalline peaks centered at $2\theta = 15^\circ$ and 20° in the XRD pattern. The rigid crystalline structure of chitosan is mainly kept via hydrogen bonding, including intermolecular and intramolecular [51].

The XRD pattern for CS: LiCO_2CH_3 plasticized with various quantities of glycerol as a plasticizer is shown in Figure 5. It is clearly seen that with increasing glycerol, the peak intensity decreases, and the broadness increases. Earlier studies have confirmed that plasticizer incorporation to polymer electrolytes is helpful for increasing both the conductivity and the amorphous phase [5,8,11]. Plasticizers also reduce the number of active centers, thereby weakening the intermolecular and intramolecular forces between the polymer chains. Consequently, the reduction in the degree of crystallinity makes the salt dissociation capability to be guaranteed, and as a consequence, an enhancement of charge carrier transport occurs [11]. Based on these observations, the increase in DC conductivity observed in impedance analysis (see Table 1) may be related to the increase in amorphous as well as the dissociation of salts.

3.4. TNM Study

The transference number measurement (TNM) is performed to evaluate the conductivity of the glycerolized system. Figure 6 exhibits the plot of current against time during polarization for the relatively high conducting electrolyte (CSGL 3). Shukur et al. [54] stated that the ionic conductivity within the polymer electrolyte system is responded by ions if the transference number of ion (t_{ion}) is

close to unity. The transference number of the ion and electron (t_{el}) is calculated using the following Equations [55].

$$t_{ion} = \frac{I_i - I_{ss}}{I_i} \tag{9}$$

$$t_{el} = 1 - t_{ion} \tag{10}$$

where I_i and I_{ss} represent the current at initial and steady-state, respectively.

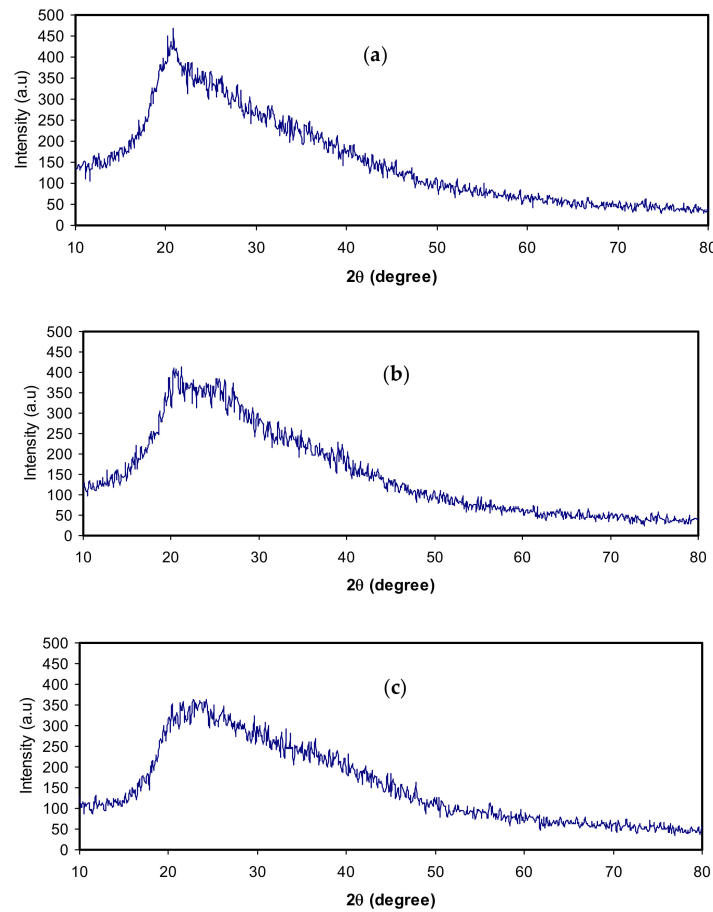


Figure 5. XRD pattern for (a) CSGL 1, (b) CSGL 2, and (c) CSGL 3.

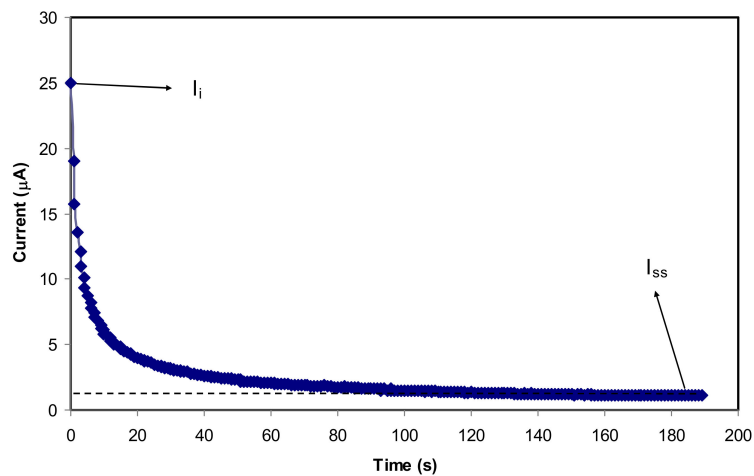


Figure 6. Current versus time for the highest conducting electrolyte.

Figure 6 shows current time transient, where the initial current decreases over electrochemical course due to the decrease in ionic species in the electrolyte and reaches a steady state when it is completely reduced [56]. Under steady-state conditions, the movement of mobile ions is balanced by the diffusion process [56]. Rani et al. [57] stated that during the polarization process, the stainless steel electrodes are responsible for the current flow blocking of ions as a result of the passing of electrons only through the solid metallic electrodes.

Using Equations (9) and (10), the values of t_{ion} and t_{el} for the electrolyte under study are 0.956 and 0.044, respectively. This result indicates the dominance of ions for conducting in this electrolyte. Mohan et al. [58] reported that a high t_{ion} value of 0.98 was obtained for a relatively high conducting electrolyte in the poly (vinyl chloride) (PVC)—poly (ethyl methacrylate) (PEMA)—sodium perchlorate (NaClO_4) system. Shukur et al. [59] reported that the plasticized system of chitosan-ammonium bromide (NH_4Br) gave the t_{ion} and t_{el} values of 0.98 and 0.02, respectively. Thus, the present results for the electrolyte system are comparable to those reported in the literature. However, in the previous reports [60,61], the low values of the transference number of Li^+ ions have been recorded for the unplasticized systems of Lithium bis (fluorosulfonyl) imide/poly (ethylene oxide) (PEO) polymer and polyacrylonitrile (PAN)/PEO/organo-modification of the SWy-2 (org-SWy) electrolytes. In our work, glycerol provides more ions for the electrolyte systems, causing an increment in the ionic transference number.

3.5. Linear Sweep Voltammetry (LSV)

The potential window of the electrolyte at room temperature can be determined from the LSV study. The LSV response from 0 to 2.5 V for the relatively high conducting electrolyte (CSGL 3) at 10 mV/s is presented in Figure 7. It is observed that there is no noticeable current flow at the potential below 1.80 V, indicating the absence of electrochemical reactions [62]. The final potential (i.e., decomposition) of the window of the electrolyte ends at 1.80 V, which is comparable with the value documented for the plasticized PEMA-based polymer electrolyte system by Anuar et al. [63]. Therefore, the decomposition potential obtained for the electrolyte under study is highly satisfactory to be applied in EDLC that normally operates at 1.0 V [64].

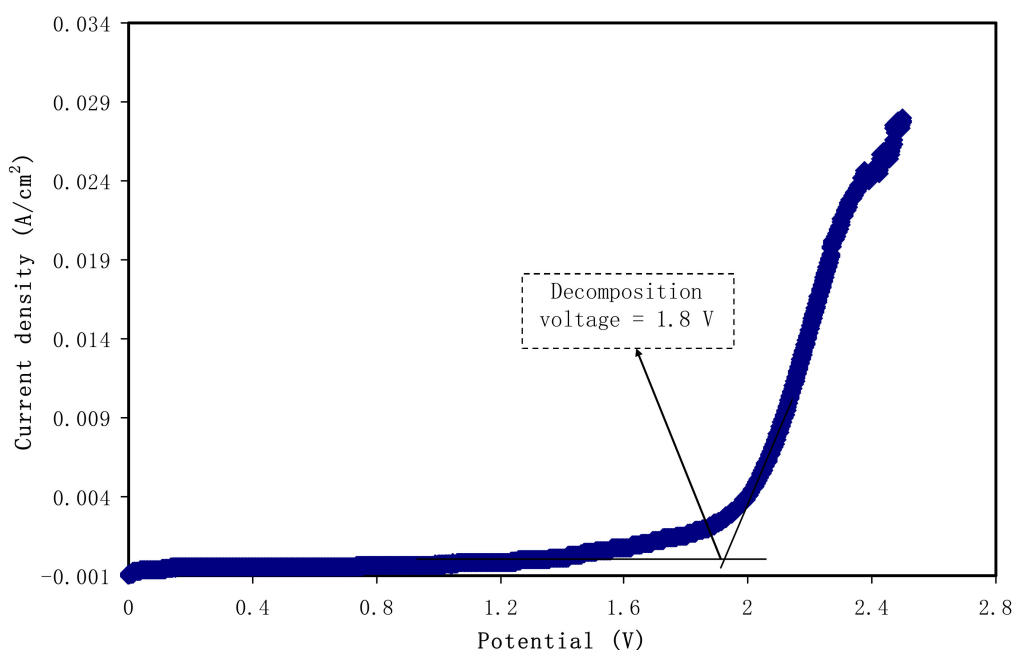


Figure 7. Linear sweep voltammetry (LSV) curve for the highest conducting electrolyte.

3.6. CV and EDLC Characterization

The cyclic voltammetry (CV) is carried out on the carbon electrode and chitosan (CS):LiCO₂CH₃:Glycerol to evaluate the capacitive behavior of the EDLC under study. The CV is carried out at different scan rates, as shown in Figure 8. It is interesting to note that the CV shape turns from leaf-shape to rectangular as the scan rate is decreased. To explain this phenomenon, the factor of the type of electrodes is crucial because the difference in internal resistance and porosity causes the shape of CV response to be an imperfect rectangular shape [65]. Of special interest, no peak is observed, suggesting no possibility of a Faradaic process (i.e., charge transfer) in the fabricated EDLC. Instead, both cations and anions in the EDLC migrate to negative and positive electrodes, respectively, during the charging process. The anion is attracted by the positive electrode, while the opposite situation occurs at the negative electrode. The high electric field holds the ions and electrons by electrolyte and electrode, respectively [66]. This indicates the development of a double-layer charge at the surface of carbon electrodes, where the energy is stored in the form of potential energy [67]. The values of C_s at each scan rate are calculated from the CVs using Equation (1) and are tabulated in Table 2.

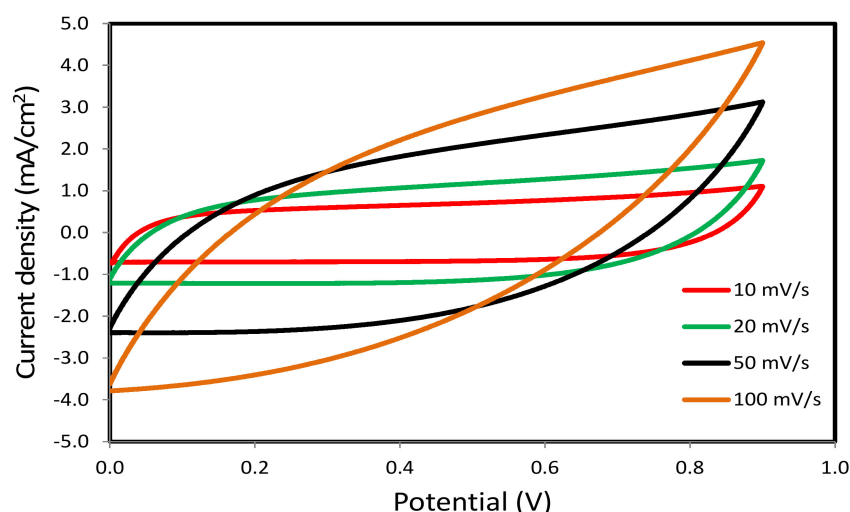


Figure 8. Cyclic voltammetry (CV) curves of the fabricated electrochemical double-layer capacitor (EDLC) at different scan rates.

Table 2. Specific capacitance (C_s) of the electrochemical double-layer capacitor (EDLC) at different scan rates.

Scan Rate (mV/s)	Specific Capacitance, C_s (F/g)
10	77.36
20	60.73
50	37.85
100	21.89

As the scan rate is increased, the C_s value is seen to decrease. It results in lowering the number of stored charges on the surface of the electrodes at a high scan rate, which, in turn, results in the increment of energy loss and decrease in the C_s values [68]. To examine the charge-discharge process in the EDLC under the study, the galvanostatic technique is applied. Figure 9 exhibits the charge-discharge profile of the EDLC on the carbon electrode and chitosan (CS):LiCO₂CH₃:Glycerol. The linear capacitive behavior in the EDLC is verified via the discharge slope [52]. The C_s of the EDLC from charge-discharge curves is calculated using Equation (2).

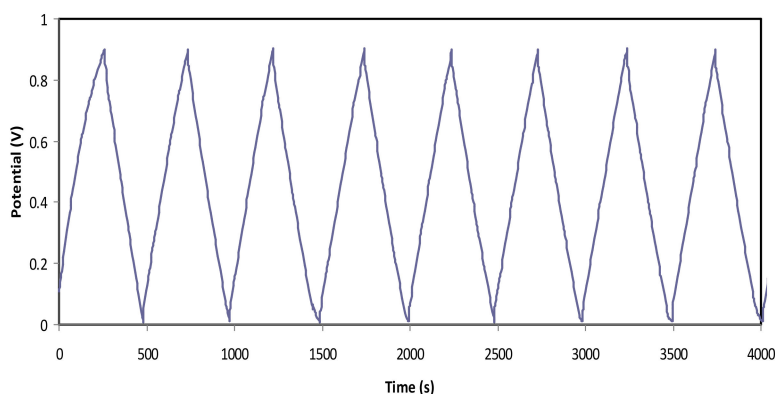


Figure 9. Charge-discharge profile for the fabricated EDLC device.

Figure 10 shows the calculated C_s values of the EDLC over a long electrochemical course of 700 cycles. At the 1st cycle, the C_s is found to be 105.5 F/g, which is slightly different compared to that extracted from CV analysis, which proves that EDLC exhibits the characteristics of the capacitor cell [69]. At the 400th cycle, the C_s increases to 132.8 F/g and becomes almost constant at an average value of 136.8 F/g up to the 700th cycle. An incredibly interesting observation is that the C_s obtained in this study is comparable to the C_s value for the fabricated EDLC, which was at ~130 F/g, as documented by Yadav et al. [70]. Consequently, it is suitable to use plasticized chitosan (CS):LiCO₂CH₃:Glycerol electrolyte as a new material in the fabrication of EDLC with high specific capacitance. It is also critical to know the columbic efficiency (η) parameter regarding the cycling stability of the EDLC, where it is calculated from the following Equation [13].

$$\eta = \frac{t_d}{t_c} \times 100 \tag{11}$$

where t_d and t_c are the discharge and charge time, respectively. Figure 10 shows the efficiency of the fabricated EDLC, where plasticized chitosan (CS):LiCO₂CH₃:Glycerol is used over 700 cycles. At the 1st cycle, the efficiency is found to be 84.6% and increases to 91.4% at the 10th cycle. Importantly, at the 30th cycle, the efficiency is observed to be 98.8% and then kept constant at ~99.5% up to 700 cycles. This indicates plausible electrode-electrolyte contact as the efficiency is higher than 90.0% EDLC under study [71].

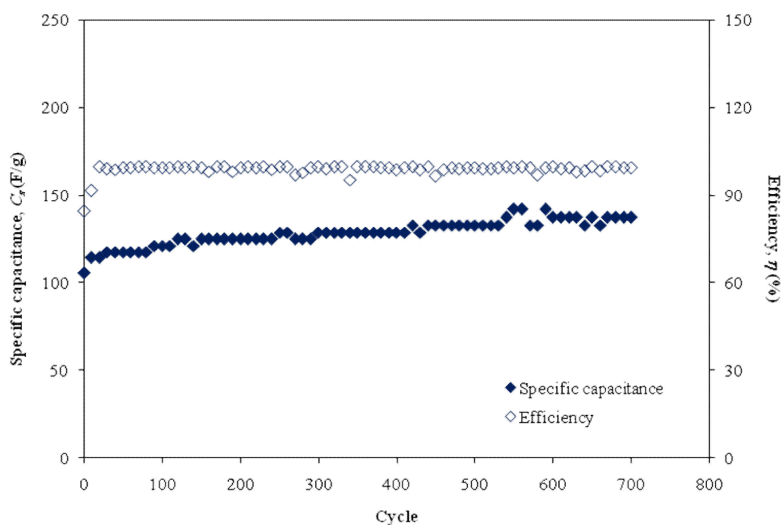


Figure 10. Specific capacitance, C_s , and efficiency, η , of the fabricated EDLC for 700 cycles.

From the charge-discharge profile in Figure 9, there are tiny potential drops (V_d) before the discharging process begins. This can be related to the existence of internal resistance in the EDLC, which is called equivalent series resistance (*ESR*). This *ESR* of the EDLC can be obtained from Equation (3). Figure 11 exhibits the *ESR* of the EDLC for 700 cycles. It can be determined that the *ESR* value varies from 40 to 75 Ω over 700 cycles, and it is noticeable that the value is slightly increased with a positive slope throughout the 700 cycles. As mentioned by Arof et al. [72], the internal resistance exists due to the charge and discharge process of electrolytes, type of current collectors (aluminum foils), and also the gap between electrolyte and electrode. The small value of *ESR* portrays good contact between the electrode and the electrolyte and indicates that it is easy for ions to migrate toward the surface of the electrode to form an electrical double-layer [73]. A similar trend is observed for the starch-lithium acetate system, where the *ESR* is slightly increased when the C_s remains at a constant value [74]. Besides, the rapid charging and discharging process will lead to the recombination of free ions, and then the ion pair will be developed, which leads to the conductivity decrement. Kang et al. [75] also stated that *ESR* is strongly related to the conductivity of an electrolyte.

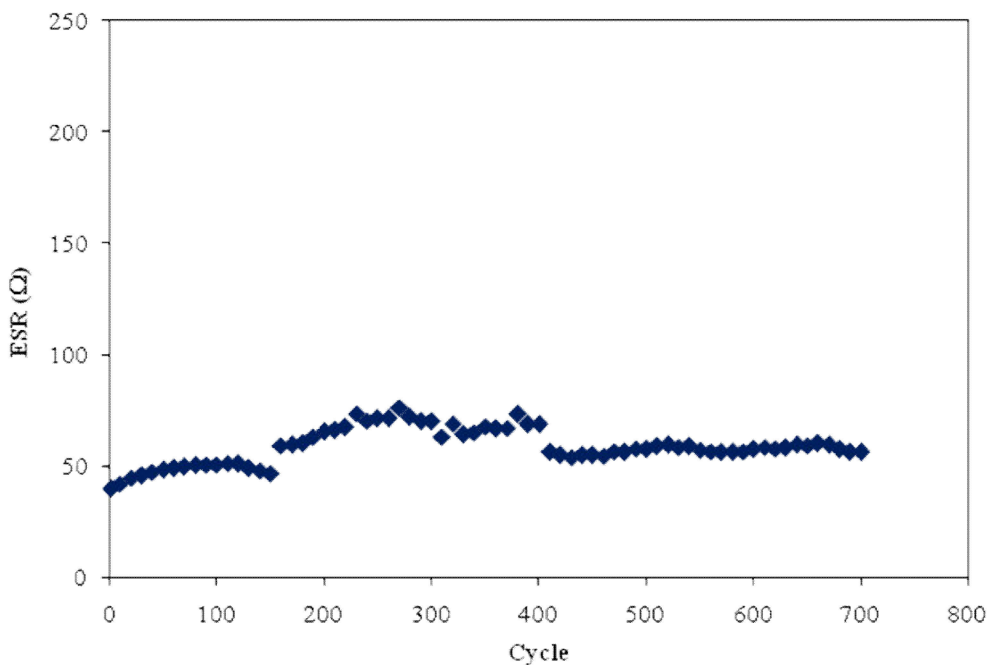


Figure 11. Equivalent series resistance (*ESR*) of the fabricated EDLC for 700 cycles.

The energy density (E) and power density (P) are also important to describe the performance of the EDLC. These parameters can be expressed by using the following Equations [76].

$$E = \frac{C_s V^2}{2} \tag{12}$$

$$P = \frac{V^2}{4m(ESR)} \tag{13}$$

Figure 12 exhibits the calculated energy density for 700 cycles. The EDLC obtains the energy density (E) of 14.7 Wh/kg at the 1st cycle, and the value is gradually increased to 18.4 Wh/kg at the 450th cycle and then kept stable at 19.1 Wh/kg from 540th cycle towards the final cycle. This trend is harmonized with the pattern of C_s illustrated in Figure 10. This result explains that the charge carriers require almost the same amount of energy to migrate towards the surface of the electrodes for the entire process of charge and discharge [77]. The results of the present work reveal that biopolymer-based electrolytes are crucial for energy storage applications. Previous studies have

indicated that biopolymer-based electrolytes have been widely utilized in electrochemical devices, such as EDLC and batteries [78–82], but their electrochemical performances are still low. In the present work, high energy density (19.1 Wh/kg) is obtained, which can be considered as a new approach in this field. EDLCs are devices, which can occupy the spaces between electrochemical batteries and electrostatic capacitors with regard to energy density and power density [83]. The achieved energy density in the current work is 19.1 Wh/kg, which is in the range of the energy density of batteries (see Figure 13). Thus, the challenges in this field of study (EDLC study) are to design EDLC devices with an energy density close enough to batteries in addition to its high power density. Moreover, the power density (P) values are calculated by using Equation (13) for selected cycles, where P value at the 1st cycle is found to be 2.591×10^3 W/kg (see Figure 14). Then, it is dropped to 1830.6 W/kg at the 400th cycle and has remained constant until the EDLC has completed 700 cycles. The trend of P is in agreement with the trend of the ESR plot. This is because the depletion of electrolytes occurs when the internal resistance increases, causing the recombination of ions due to the fast charging and discharging mechanism, thus resulting in reduced P at a high cycle number [84]. Both E and P values are clearly dependent on the mass loading of active material in the fabrication of EDLC. The low mass loading and relatively low current are reported to be responsible for providing enhanced electrochemical performance [85].

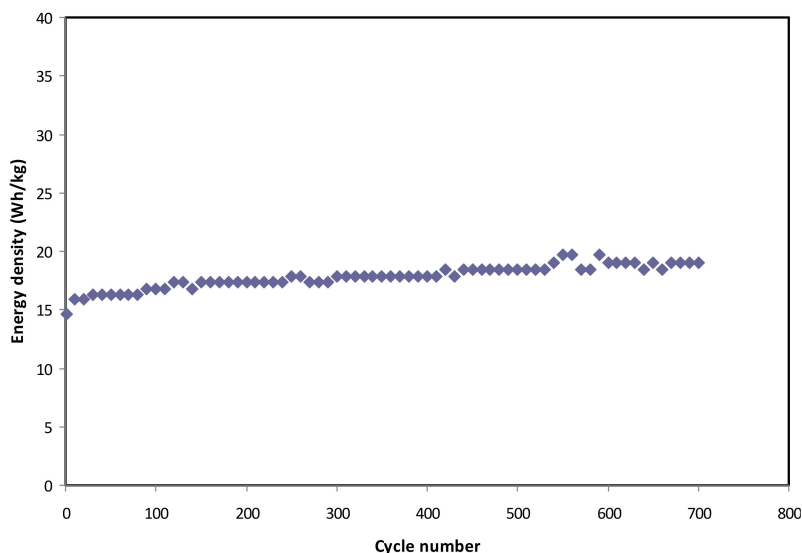


Figure 12. Energy density, E , of the fabricated EDLC for 700 cycles.

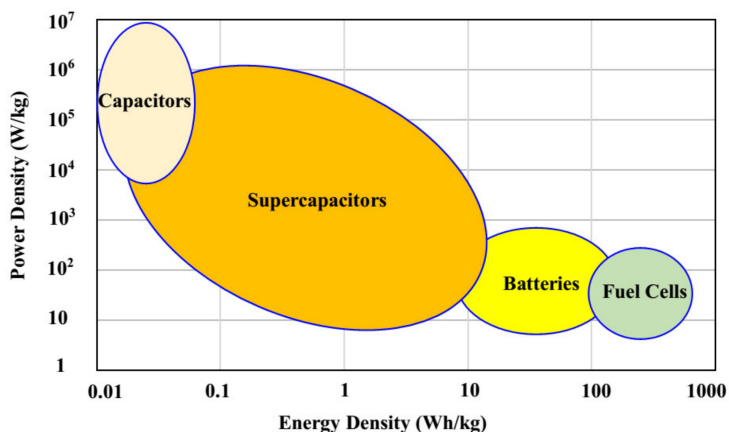


Figure 13. Ragone plot of energy density versus power density for numerous electrical energy storage and conversion devices [83].

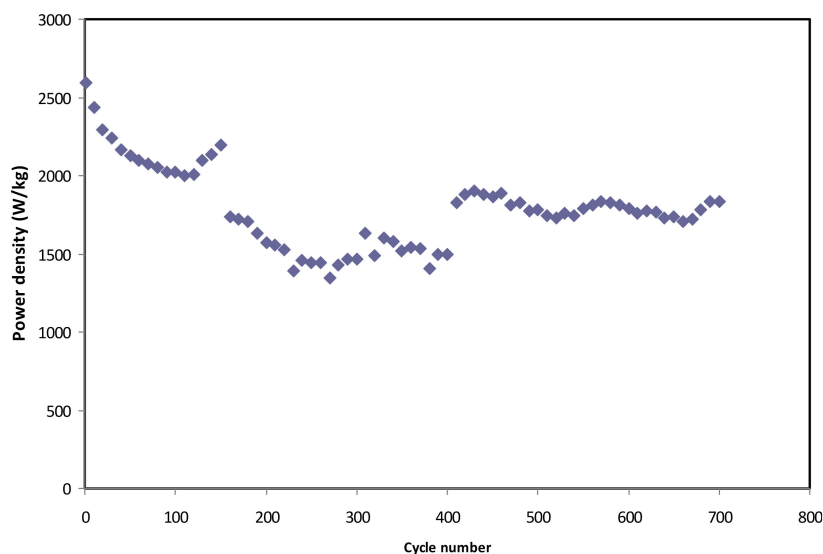


Figure 14. The power density of the fabricated EDLC for 100 cycles.

4. Conclusions

Chitosan (CS):LiCO₂CH₃:Glycerol polymer electrolytes were prepared with a solution cast method. The electrolyte studied in this current work could be established as new materials in the fabrication of EDLC with high specific capacitance, energy density, and power density. The dielectric properties were correlated with DC conductivity to understand the conductivity behavior of the plasticized electrolytes. The system with high dielectric constant was also associated with high DC conductivity ($5.19 \times 10^{-4} \text{ Scm}^{-1}$). The reduction of crystallinity and increase of DC conductivity upon the addition of glycerol were ascribed to the disruption of intermolecular hydrogen bonds and dissociation of more salts through the electrolyte. Li⁺ and CH₃CO₂⁻ ions were the main charge carriers throughout the conduction process rather than electrons as t_{el} was less than t_{ion} . These relatively high values of both ion transference number and potential stability confirmed the possibility of the fabricated systems for the electrochemical device as energy storage. The sharp drop in the current value of the TNM plot verified that the CS:LiCO₂CH₃:Glycerol was an ionic conductor. From CV analysis, it was found that the specific capacitance reduced from 77.36 F/g to 21.89 F/g as the scan rate changed from 10 mV/s to 100 mV/s, respectively. The capacitive characteristic of the fabricated EDLC was confirmed as no redox peaks were observed in the CV plot, as well as the linearity of the discharge curve. The EDLC was stable up to 700 cycles, where the efficiency was stable from 98.8% to 99.5%. Ions in CS:LiCO₂CH₃:Glycerol was considered to have almost the same energy barrier during the conduction process as the energy density (average $E = 18.4 \text{ Wh/kg}$) was almost constant throughout 700 cycles. The specific capacitance of the EDLC was 132.8 F/g. The power density of the EDLC was quite high (2591 W/kg). This could be due to the low value of ESR, which was 40 Ω.

Author Contributions: Conceptualization, S.B.A., Y.M.Y., and M.F.Z.K.; Formal analysis, A.S.F.M.A.; Funding acquisition, M.M.N.; Investigation, S.B.A. and M.H.H.; Methodology, S.B.A. and M.A.B.; Project administration, S.B.A. and M.M.N.; Supervision, S.B.A.; Validation, M.M.N., M.H.H., M.A.B., Y.M.Y., R.T.A., S.K.M., and M.F.Z.K.; Writing—original draft, A.S.F.M.A. and S.B.A.; Writing—review and editing, M.M.N., M.H.H., M.A.B., Y.M.Y., R.T.A., S.K.M., and M.F.Z.K. All authors have read and agreed to the published version of the manuscript.

Funding: The authors gratefully acknowledge the financial support for this study from the Ministry of Higher Education and Scientific Research-Kurdish National Research Council (KNRC), Kurdistan Regional Government/Iraq. The financial support from Prince Sultan University is greatly acknowledged.

Acknowledgments: The authors gratefully acknowledge the financial support for this study from the Ministry of Higher Education and Scientific Research-Kurdish National Research Council (KNRC), Kurdistan Regional Government/Iraq. The financial support from the University of Sulaimani and Komar University of Science and Technology are greatly appreciated.

Conflicts of Interest: The authors declare no conflicts of interest.

References

1. Huanhuan, W.; Jianyi, L.; Ze, X.S. Polyaniline (PANi) based electrode materials for energy storage and conversion. *J. Sci. Adv. Mater. Devices* **2016**, *1*, 225–255.
2. Aziz, S.B.; Hamsan, M.H.; Kadir, M.F.Z.; Karim, W.O.; Abdullah, R.M. Development of polymer blend electrolyte membranes based on chitosan: Dextran with high ion transport properties for EDLC application. *Int. J. Mol. Sci.* **2019**, *20*, 3369. [[CrossRef](#)]
3. Inagaki, M.; Konno, H.; Tanaike, O. Carbon materials for electrochemical capacitors. *J. Power Sources* **2010**, *195*, 7880–7903. [[CrossRef](#)]
4. Zhang, D.; Zhang, X.; Chen, Y.; Yu, P.; Wang, C.; Ma, Y. Enhanced capacitance and rate capability of graphene/polypyrrole composite as electrode material for supercapacitors. *J. Power Sources* **2011**, *196*, 5990–5996. [[CrossRef](#)]
5. Shukur, M.F.; Ithnin, R.; Illias, H.A.; Kadir, M.F.Z. Proton conducting polymer electrolyte based on plasticized chitosan-PEO blend and application in electrochemical devices. *Opt. Mater. (Amst.)* **2013**, *35*, 1834–1841. [[CrossRef](#)]
6. Ling, L.; Qing-Han, M. Electrochemical properties of mesoporous carbon aerogel electrodes for electric double layer capacitors. *J. Mater. Sci.* **2005**, *40*, 4105–4107. [[CrossRef](#)]
7. Subramanian, V.; Zhu, H.; Wei, B. Nanostructured manganese oxides and their composites with carbon nanotubes as electrode materials for energy storage devices. *Pure Appl. Chem.* **2008**, *80*, 2327–2343. [[CrossRef](#)]
8. Kadir, M.F.Z.; Majid, S.R.; Arof, A.K. Plasticized chitosan-PVA blend polymer electrolyte based proton battery. *Electrochim. Acta* **2010**, *55*, 1475–1482. [[CrossRef](#)]
9. Aziz, S.B.; Muhamad, H.H.; Muaffaq, M.N.; Wrya, O.K.; Iver, B.; Mohamad, A.B.; Rebar, T.A.; Al-Zangana, S.; Kadir, M.F.Z. Structural, Impedance and Electrochemical Characteristics of Electrical Double Layer Capacitor Devices Based on Chitosan: Dextran Biopolymer Blend Electrolytes. *Polymers* **2020**, *12*, 1411. [[CrossRef](#)]
10. Ibrahim, S.; Mohd Yasin, S.M.; Nee, N.M.; Ahmad, R.; Johan, M.R. Conductivity and dielectric behaviour of PEO-based solid nanocomposite polymer electrolytes. *Solid State Commun.* **2012**, *152*, 426–434. [[CrossRef](#)]
11. Aziz, S.B.; Woo, T.J.; Kadir, M.F.Z.; Ahmed, H.M. A conceptual review on polymer electrolytes and ion transport models. *J. Sci. Adv. Mater. Devices* **2018**, *3*, 1–17. [[CrossRef](#)]
12. Gupta, S.; Varshney, P.K. Effect of plasticizer concentration on structural and electrical properties of hydroxyethyl cellulose (HEC)-based polymer electrolyte. *Ionics (Kiel)* **2017**, *23*, 1613–1617. [[CrossRef](#)]
13. Hamsan, M.H.; Aziz, S.B.; Azha, M.A.S.; Azli, A.A.; Shukur, M.F.; Yusof, Y.M.; Muzakir, S.K.; Manan, N.S.A.; Kadir, M.F.Z. Solid-state double layer capacitors and protonic cell fabricated with dextran from *Leuconostoc mesenteroides* based green polymer electrolyte. *Mater. Chem. Phys.* **2019**, 1–55. [[CrossRef](#)]
14. Sekhar, P.C. Effect of plasticizer on conductivity and cell parameters of (PMMA+NaClO₄) polymer electrolyte system. *IOSR J. Appl. Phys.* **2012**, *2*, 1–6. [[CrossRef](#)]
15. Buraidah, M.H.; Shah, S.; Teo, L.P.; Chowdhury, F.I.; Careem, M.A.; Albinsson, I.; Mellander, B.E.; Arof, A.K. High efficient dye sensitized solar cells using phthaloylchitosan based gel polymer electrolytes. *Electrochim. Acta* **2017**, *245*, 846–853. [[CrossRef](#)]
16. Isa, K.B.M. Magnesium ion-based gel polymer electrolytes: Ionic conduction and infrared spectroscopy studies. *Int. J. Electrochem. Sci.* **2013**, *8*, 3602–3614.
17. Riess, I. Polymeric mixed ionic electronic conductors. *Solid State Ionics* **2000**, *136*, 1119–1130. [[CrossRef](#)]
18. Nyuk, C.M.; Mohd Isa, M.I.N. Solid biopolymer electrolytes based on carboxymethyl cellulose for use in coin cell proton batteries. *J. Sustain. Sci. Manag.* **2017**, *2017*, 42–48.
19. Salleh, N.S.; Aziz, S.B.; Aspanut, Z.; Kadir, M.F.Z. Electrical impedance and conduction mechanism analysis of biopolymer electrolytes based on methyl cellulose doped with ammonium iodide. *Ionics (Kiel)* **2016**, *22*, 2157–2167. [[CrossRef](#)]
20. Hamsan, M.H.; Aziz, S.B.; Shukur, M.F.; Kadir, M.F.Z. Protonic cell performance employing electrolytes based on plasticized methylcellulose-potato starch-NH₄NO₃. *Ionics (Kiel)* **2019**, *25*, 559–572. [[CrossRef](#)]
21. Stepniak, I.; Galinski, M.; Nowacki, K.; Wysokowski, M.; Jakubowska, P.; Bazhenov, V.V.; Leisegang, T.; Ehrlich, H.; Jesionowski, T. A novel chitosan/sponge chitin origin material as a membrane for supercapacitors-preparation and characterization. *RSC Adv.* **2016**, *6*, 4007–4013. [[CrossRef](#)]

22. Hassan, M.F.; Azimi, N.S.N.; Kamarudin, K.H.; Sheng, C.K. Solid polymer electrolytes based on starch-Magnesium Sulphate: Study on morphology and electrical conductivity. *ASM Sci. J.* **2018**, *11*, 17–28.
23. Rayung, M.; Aung, M.M.; Azhar, S.C.; Abdullah, L.C.; Su'ait, M.S.; Ahmad, A.; Jamil, S.N.A.M. Bio-Based Polymer Electrolytes for Electrochemical Devices: Insight into the Ionic Conductivity Performance. *Materials* **2020**, *13*, 838. [[CrossRef](#)] [[PubMed](#)]
24. Moniha, V.; Alagar, M.; Selvasekarapandian, S.; Sundaresan, B.; Hemalatha, R.; Boopathi, G. Synthesis and characterization of bio-polymer electrolyte based on iota-carrageenan with ammonium thiocyanate and its applications. *J. Solid State Electrochem.* **2018**, *22*, 3209–3223. [[CrossRef](#)]
25. Thakur, V.K.; Thakur, M.K. Recent advances in graft copolymerization and applications of chitosan: A review. *ACS Sustain. Chem. Eng.* **2014**, *2*, 2637–2652. [[CrossRef](#)]
26. Du, B.W.; Hu, S.Y.; Singh, R.; Tsai, T.T.; Lin, C.C.; Ko, F.H. Eco-friendly and biodegradable biopolymer chitosan/Y₂O₃ composite materials in flexible organic thin-film transistors. *Materials (Basel)* **2017**, *10*, 1026. [[CrossRef](#)]
27. Hamsan, M.H.; Shukur, M.F.; Aziz, S.B.; Yusof, Y.M.; Kadir, M.F.Z. Influence of NH₄Br as an ionic source on the structural/electrical properties of dextran-based biopolymer electrolytes and EDLC application. *Bull. Mater. Sci.* **2019**, *43*. [[CrossRef](#)]
28. Aziz, S.B.; Brza, M.A.; Hamsan, M.H.; Kadir, M.F.Z.; Muzakir, S.K.; Abdulwahid, R.T. Effect of ohmic-drop on electrochemical performance of EDLC fabricated from PVA:dextran:NH₄I based polymer blend electrolytes. *J. Mater. Res. Technol.* **2020**, *9*, 3734–3745. [[CrossRef](#)]
29. Aziz, S.B.; Brza, M.A.; Mishra, K.; Hamsan, M.H.; Karim, W.O.; Abdullah, R.M.; Abdulwahid, R.T. Fabrication of high performance energy storage EDLC device from proton conducting methylcellulose: Dextran polymer blend electrolytes. *J. Mater. Res. Technol.* **2019**, *9*, 1137–1150. [[CrossRef](#)]
30. Deraman, S.K.; Mohamed, N.S.; Subban, R.H.Y. Ionic liquid incorporated PVC based polymer electrolytes: Electrical and dielectric properties. *Sains Malays.* **2014**, *43*, 877–883.
31. Aziz, S.B.; Hamsan, M.H.; Kadir, M.F.Z.; Woo, H.J. Design of Polymer Blends Based on Chitosan:POZ with Improved Dielectric Constant for Application in Polymer Electrolytes and Flexible Electronics. *Adv. Polym. Technol.* **2020**, *2020*, 1–10. [[CrossRef](#)]
32. Jihad, M.H.; Aziz, S.B.; Mustafa, M.S.; Brza, M.A.; Hamsan, M.H.; Kadir, M.F.Z.; Ghareeb, H.O.; Hussein, S.A. Electrochemical Impedance study of Proton Conducting Polymer Electrolytes based on PVC Doped with Thiocyanate and Plasticized with Glycerol. *Int. J. Electrochem. Sci.* **2020**, *15*, 4671–4683. [[CrossRef](#)]
33. Marf, A.S.; Abdullah, R.M.; Aziz, S.B. Structural morphological, electrical and electrochemical properties of PVA: CS-Based Proton-conducting polymer blend electrolytes. *Membranes* **2020**, *10*, 71. [[CrossRef](#)] [[PubMed](#)]
34. Aziz, S.B.; Brza, M.A.; Saed, S.R.; Hamsan, M.H.; Kadir, M.F.Z. Ion association as a main shortcoming in polymer blend electrolytes based on CS:PS incorporated with various amounts of ammonium tetrafluoroborate. *J. Mater. Res. Technol.* **2020**, *9*, 5410–5421. [[CrossRef](#)]
35. Salman, Y.A.; Abdullah, O.G.; Hanna, R.R.; Aziz, S.B. Conductivity and electrical properties of chitosan-methylcellulose blend biopolymer electrolyte incorporated with lithium tetrafluoroborate. *Int. J. Electrochem. Sci.* **2018**, *13*, 3185–3199. [[CrossRef](#)]
36. Chan, C.H.; Kammer, H.-W. Impedance spectra of polymer electrolytes. *Ionics* **2017**, *23*, 2327–2337. [[CrossRef](#)]
37. Aziz, S.B.; Brza, M.A.; Mohamed, P.A.; Kadir, M.F.Z.; Hamsan, M.H.; Abdulwahid, R.T.; Woo, H.J. Increase of Metallic Silver Nanoparticles in Chitosan:AgNt Based Polymer Electrolytes Incorporated with Alumina Filler. *Results Phys.* **2019**, 102326. [[CrossRef](#)]
38. Ramya, C.S.; Selvasekarapandian, S.; Hirankumar, G.; Savitha, T.; Angelo, P.C. Investigation on dielectric relaxations of PVP–NH₄SCN polymer electrolyte. *J. Non-Cryst. Solids* **2008**, *354*, 1494–1502. [[CrossRef](#)]
39. Aziz, S.B. Li⁺ ion conduction mechanism in poly (ε-caprolactone)-based polymer electrolyte. *Iran. Polym. J.* **2013**, *22*, 877. [[CrossRef](#)]
40. Aziz, S.B.; Abidin, Z.H.Z. Ion-transport study in nanocomposite solid polymer electrolytes based on chitosan: Electrical and dielectric analysis. *J. Appl. Polym. Sci.* **2015**, *132*, 41774. [[CrossRef](#)]
41. Aziz, S.B.; Kadir, M.F.Z.; Abidin, Z.H.Z. Structural, morphological and electrochemical impedance study of CS: LiTf based solid polymer electrolyte: Reformulated Arrhenius equation for ion transport study. *Int. J. Electrochem. Sci.* **2016**, *11*, 9228–9244. [[CrossRef](#)]

42. Nasef, M.M.; Saidi, H.; Dahlan, K.Z.M. Preparation of composite polymer electrolytes by electron beam-induced grafting: Proton- and lithium ion-conducting membranes. *Nucl. Instrum. Methods Phys. Res. Sect. B Beam Interact. Mater. Atoms* **2007**, *265*, 168–172. [[CrossRef](#)]
43. Aziz, S.B.; Abdullah, R.M. Crystalline and amorphous phase identification from the $\tan\delta$ relaxation peaks and impedance plots in polymer blend electrolytes based on [CS: AgNt] x: PEO (x-1)(10 ≤ x ≤ 50). *Electrochim. Acta* **2018**, *285*, 30–46. [[CrossRef](#)]
44. Aziz, S.B.; Abdullah, R.M.; Kadir, M.F.Z.; Ahmed, H.M. Non suitability of silver ion conducting polymer electrolytes based on chitosan mediated by barium titanate (BaTiO₃) for electrochemical device applications. *Electrochim. Acta* **2019**, *296*, 494–507. [[CrossRef](#)]
45. Venkateswarlu, M.; Satyanarayana, N. AC conductivity studies of silver based fast ion conducting glassy materials for solid state batteries. *Mater. Sci. Eng. B* **1998**, *54*, 189–195. [[CrossRef](#)]
46. Aziz, S.B.; Abidin, Z.H.Z.; Arof, A.K. Influence of silver ion reduction on electrical modulus parameters of solid polymer electrolyte based on chitosan-silver triflate electrolyte membrane. *Express Polym. Lett.* **2010**, *4*, 300–310. [[CrossRef](#)]
47. Jacob, M.M.E.; Prabaharan, S.R.S.; Radhakrishna, S. Effect of PEO addition on the electrolytic and thermal properties of PVDF-LiClO₄ polymer electrolytes. *Solid State Ionics* **1997**, *104*, 267–276. [[CrossRef](#)]
48. Fonseca, C.P., Jr.; Cavalcante, F.; Amaral, F.A.; Souza, C.A.Z.; Neves, S. Thermal and Conduction Properties of a PCL-biodegradable Gel Polymer Electrolyte with LiClO₄, LiF₃CSO₃, and LiBF₄ Salts. *Int. J. Electrochem. Sci.* **2007**, *2*, 52–63.
49. Mustafa, M.S.; Ghareeb, H.O.; Aziz, S.B.; Brza, M.A.; Al-Zangana, S.; Hadi, J.M.; Kadir, M.F.Z. Electrochemical characteristics of glycerolized PEO-based polymer electrolytes. *Membranes* **2020**, *10*, 116. [[CrossRef](#)]
50. Aziz, S.B.; Abidin, Z.H.Z.; Arof, A.K. Effect of silver nanoparticles on the DC conductivity in chitosan—Silver triflate polymer electrolyte. *Phys. B Phys. Condens. Matter* **2010**, *405*, 4429–4433. [[CrossRef](#)]
51. Aziz, S.B.; Hamsan, M.H.; Brza, M.A.; Kadir, M.F.Z.; Abdulwahid, R.T.; Ghareeb, H.O.; Woo, H.J. Fabrication of energy storage EDLC device based on CS: PEO polymer blend electrolytes with high Li⁺ ion transference number. *Results Phys.* **2019**, *15*, 102584. [[CrossRef](#)]
52. Aziz, S.B.; Hamsan, M.H.; Abdullah, R.M.; Kadir, M.F.Z. A Promising polymer blend electrolytes based on chitosan: Methyl cellulose for EDLC application with high specific capacitance and energy density. *Molecules* **2019**, *24*, 2503. [[CrossRef](#)] [[PubMed](#)]
53. Aziz, S.B.; Abdulwahid, R.T.; Hamsan, M.H.; Brza, M.A.; Abdullah, R.M.; Kadir, M.F.Z.; Muzakir, S.K. Structural, Impedance, and EDLC Characteristics of Proton Conducting Chitosan-Based Polymer Blend Electrolytes with High Electrochemical Stability. *Molecules* **2019**, *24*, 3508. [[CrossRef](#)] [[PubMed](#)]
54. Shukur, M.F.; Ithnin, R.; Kadir, M.F.Z. Ionic conductivity and dielectric properties of potato starch-magnesium acetate biopolymer electrolytes: The effect of glycerol and 1-butyl-3-methylimidazolium chloride. *Ionics (Kiel)* **2016**, *22*, 1113–1123. [[CrossRef](#)]
55. Aziz, S.B.; Hamsan, M.H.; Karim, W.O.; Marif, A.S.; Abdulwahid, R.T.; Kadir, M.F.Z.; Brza, M.A. Study of impedance and solid-state double-layer capacitor behavior of proton (H⁺)-conducting polymer blend electrolyte-based CS:PS polymers. *Ionics* **2020**. [[CrossRef](#)]
56. Shukur, M.F.; Ithnin, R.; Kadir, M.F.Z. Protonic Transport Analysis of Starch-Chitosan Blend Based Electrolytes and Application in Electrochemical Device. *Mol. Cryst. Liq. Cryst.* **2014**, *603*, 52–65. [[CrossRef](#)]
57. Rani, M.S.A.; Ahmad, A.; Mohamed, N.S. Influence of nano-sized fumed silica on physicochemical and electrochemical properties of cellulose derivatives-ionic liquid biopolymer electrolytes. *Ionics (Kiel)* **2018**, *24*, 807–814. [[CrossRef](#)]
58. Rama Mohan, K.; Achari, V.B.S.; Rao, V.V.R.N.; Sharma, A.K. Electrical and optical properties of (PEMA/PVC) polymer blend electrolyte doped with NaClO₄. *Polym. Test.* **2011**, *30*, 881–886. [[CrossRef](#)]
59. Shukur, M.F.; Hamsan, M.H.; Kadir, M.F.Z. Investigation of plasticized ionic conductor based on chitosan and ammonium bromide for EDLC application. *Mater. Today Proc.* **2019**, *17*, 490–498. [[CrossRef](#)]
60. Zhang, H.; Liu, C.; Zheng, L.; Xu, F.; Feng, W.; Li, H.; Huang, X.; Armand, M.; Nie, J.; Zhou, Z. Lithium bis(fluorosulfonyl)imide/poly(ethylene oxide) polymer electrolyte. *Electrochim. Acta* **2014**, *133*, 529–538. [[CrossRef](#)]
61. Simari, C.; Lufrano, E.; Coppola, L.; Nicotera, I. Composite gel polymer electrolytes based on organo-modified nanoclays: Investigation on lithium-ion transport and mechanical properties. *Membranes (Basel)* **2018**, *8*, 69. [[CrossRef](#)] [[PubMed](#)]

62. Sampathkumar, L.; Christopher Selvin, P.; Selvasekarapandian, S.; Perumal, P.; Chitra, R.; Muthukrishnan, M. Synthesis and characterization of biopolymer electrolyte based on tamarind seed polysaccharide, lithium perchlorate and ethylene carbonate for electrochemical applications. *Ionics (Kiel)* **2019**, *25*, 1067–1082. [[CrossRef](#)]
63. Anuar, N.K.; Subban, R.H.Y.; Mohamed, N.S. Properties of PEMA-NH₄CF₃SO₃ added to BMATSFI ionic liquid. *Materials (Basel)* **2012**, *5*, 2609–2620. [[CrossRef](#)]
64. Shuhaimi, N.E.A.; Alias, N.A.; Majid, S.R.; Arof, A.K. Electrical Double Layer Capacitor With Proton Conducting K-Carrageenan–Chitosan Electrolytes. *Funct. Mater. Lett.* **2009**, *1*, 195–201. [[CrossRef](#)]
65. Bandaranayake, C.M.; Weerasinghe, W.A.D.S.S.; Vidanapathirana, K.P.; Perera, K.S. A Cyclic Voltammetry study of a gel polymer electrolyte based redox-capacitor. *Sri Lankan J. Phys.* **2016**, *16*, 19. [[CrossRef](#)]
66. Kadir, M.F.Z.; Arof, A.K. Application of PVA–chitosan blend polymer electrolyte membrane in electrical double layer capacitor. *Mater. Res. Innov.* **2013**, *15*, S217–S220. [[CrossRef](#)]
67. Fattah, N.F.A.; Ng, H.M.; Mahipal, Y.K.; Numan, A.; Ramesh, S.; Ramesh, K. An approach to solid-state electrical double layer capacitors fabricated with graphene oxide-doped, ionic liquid-based solid copolymer electrolytes. *Materials (Basel)* **2016**, *9*, 450. [[CrossRef](#)]
68. Muchakayala, R.; Song, S.; Wang, J.; Fan, Y.; Benggeppagari, M.; Chen, J.; Tan, M. Development and supercapacitor application of ionic liquid-incorporated gel polymer electrolyte films. *J. Ind. Eng. Chem.* **2018**, *59*, 79–89. [[CrossRef](#)]
69. Yusof, Y.M.; Majid, N.A.; Kasmani, R.M.; Illias, H.A.; Kadir, M.F.Z. The Effect of Plasticization on Conductivity and Other Properties of Starch/Chitosan Blend Biopolymer Electrolyte Incorporated with Ammonium Iodide. *Mol. Cryst. Liq. Cryst.* **2014**, *603*, 73–88. [[CrossRef](#)]
70. Yadav, N.; Mishra, K.; Hashmi, S.A. Optimization of porous polymer electrolyte for quasi-solid-state electrical double layer supercapacitor. *Electrochim. Acta* **2017**, *235*, 570–582. [[CrossRef](#)]
71. Lim, C.S.; Teoh, K.H.; Liew, C.W.; Ramesh, S. Capacitive behavior studies on electrical double layer capacitor using poly (vinyl alcohol)-lithium perchlorate based polymer electrolyte incorporated with TiO₂. *Mater. Chem. Phys.* **2014**, *143*, 661–667. [[CrossRef](#)]
72. Arof, A.K.; Kufian, M.Z.; Syukur, M.F.; Aziz, M.F.; Abdelrahman, A.E.; Majid, S.R. Electrical double layer capacitor using poly(methyl methacrylate)-C 4BO 8Li gel polymer electrolyte and carbonaceous material from shells of mata kucing (*Dimocarpus longan*) fruit. *Electrochim. Acta* **2012**, *74*, 39–45. [[CrossRef](#)]
73. Asmara, S.N.; Kufian, M.Z.; Majid, S.R.; Arof, A.K. Preparation and characterization of magnesium ion gel polymer electrolytes for application in electrical double layer capacitors. *Electrochim. Acta* **2011**, *57*, 91–97. [[CrossRef](#)]
74. Wang, J.; Zhao, Z.; Song, S.; Ma, Q.; Liu, R. High performance poly(vinyl alcohol)-based Li-ion conducting gel polymer electrolyte films for electric double-layer capacitors. *Polymers (Basel)* **2018**, *10*, 1179. [[CrossRef](#)] [[PubMed](#)]
75. Kang, J.; Wen, J.; Jayaram, S.H.; Yu, A.; Wang, X. Development of an equivalent circuit model for electrochemical double layer capacitors (EDLCs) with distinct electrolytes. *Electrochim. Acta* **2014**, *115*, 587–598. [[CrossRef](#)]
76. Aziz, S.B.; Hamsan, M.H.; Brza, M.A.; Kadir, M.F.Z.; Muzakir, S.K.; Abdulwahid, R.T. Effect of glycerol on EDLC characteristics of chitosan: Methylcellulose polymer blend electrolytes. *J. Mater. Res. Technol.* **2020**, *9*, 8355–8366. [[CrossRef](#)]
77. Shukur, M.F.; Ithnin, R.; Kadir, M.F.Z. Electrical characterization of corn starch-LiOAc electrolytes and application in electrochemical double layer capacitor. *Electrochim. Acta* **2014**, *136*, 204–216. [[CrossRef](#)]
78. Hamsan, M.H.; Shukur, M.F.; Kadir, M.F.Z. NH₄NO₃ as charge carrier contributor in glycerolized potato starch-methyl cellulose blend-based polymer electrolyte and the application in electrochemical double-layer capacitor. *Ionics* **2017**, *23*, 3429–3453. [[CrossRef](#)]
79. Aziz, S.B.; Hamsan, M.H.; Abdullah, R.M.; Abdulwahid, R.T.; Brza, M.A.; Marif, A.S.; Kadir, M.F.Z. Protonic EDLC cell based on chitosan (CS): Methylcellulose (MC) solid polymer blend electrolytes. *Ionics* **2020**. [[CrossRef](#)]
80. Teoh, K.H.; Lim, C.; Liew, C.; Ramesh, S. Electric double-layer capacitors with corn starch-based biopolymer electrolytes incorporating silica as filler. *Ionics* **2015**, *21*, 2061–2068. [[CrossRef](#)]

81. Kadir, M.F.Z.; Salleh, N.S.; Hamsan, M.H.; Aspanut, Z.; Majid, N.A.; Shukur, M.F. Biopolymeric electrolyte based on glycerolized methyl cellulose with NH₄Br as proton source and potential application in EDLC. *Ionics* **2018**, *24*, 1651–1662. [[CrossRef](#)]
82. Tan, H.W.; Ramesh, S.; Liew, C. Electrical, thermal, and structural studies on highly conducting additive-free biopolymer electrolytes for electric double-layer capacitor application. *Ionics* **2019**, *25*, 4861–4874. [[CrossRef](#)]
83. Abbas, Q.; Raza, R.; Shabbir, I.; Olabi, A.G. Heteroatom doped high porosity carbon nanomaterials as electrodes for energy storage in electrochemical capacitors: A review. *J. Sci. Adv. Mater. Devices* **2019**, *4*, 341–352. [[CrossRef](#)]
84. Zhong, C.; Deng, Y.; Hu, W.; Qiao, J.; Zhang, L.; Zhang, J. A review of electrolyte materials and compositions for electrochemical supercapacitors. *Chem. Soc. Rev.* **2015**, *44*, 7484–7539. [[CrossRef](#)] [[PubMed](#)]
85. Muzaffar, A.; Ahamed, M.B.; Deshmukh, K.; Thirumalai, J. A review on recent advances in hybrid supercapacitors: Design, fabrication and applications. *Renew. Sustain. Energy Rev.* **2019**, *101*, 123–145. [[CrossRef](#)]



© 2020 by the authors. Licensee MDPI, Basel, Switzerland. This article is an open access article distributed under the terms and conditions of the Creative Commons Attribution (CC BY) license (<http://creativecommons.org/licenses/by/4.0/>).